https://doi.org/10.46813/2023-145-158

INFLUENCE OF HELIUM IONS BEAMS WITH ENERGIES 0.12 MeV ON SPUTTERING PROCESS ON SURFACE OF TUNGSTEN

O.V. Manuilenko[1,4], E.M. Prokhorenko[2], K.V. Pavlii[1], B.V. Zajtsev[1], S.N. Dubniuk[1], V.V. Lytvynenko[2], Yu.A. Kasatkin[2], T.G. Prokhorenko[3]
[1]NSC "Kharkov Institute of Physics and Technology", Kharkiv, Ukraine;
[2]Institute of Electrophysics and Radiation Technologies NAS of Ukraine, Kharkiv, Ukraine;
[3]Kharkiv National Automobile and Highway University, Kharkiv, Ukraine;
[4]V.N. Karazin Kharkiv National University, Kharkiv, Ukraine
E-mail: forshad58@gmail.com

The samples of tungsten with a purity of 99.5 and 99.7% were irradiated with helium ion beams (E_{He}^{+} = 0.12 MeV). The total sputtering coefficients for the sample depth up to 60 Å from the surface of sample were obtained. It was found that on the surface of tungsten, the number of pits (the flecking effect) significantly exceeds the number of bubbles (the blistering effect). The damage profiles of the surface of tungsten as a result of irradiation with helium ions are calculated. The areas of maximal display of effects of damage are determined.

PACS: 52.40.HF, 29.27Ac, 621.715:539.376, 87.55N

INTRODUCTION

The current state of the issues of creating materials for the first wall of the divertor is in the center of attention. The reason for this is that the materials of the first wall are exposed to thermal influences, to a plasma flows when a current breakdown occurs, radiation exposure by nuclear fusion products [1–3]. In all these areas, a significant amount of work has been done, and certain results have been obtained. However, there is no complete solution to the problem.

In a fusion reactor, the first wall is exposed to high temperature (>1200 K). Exposure to high temperature leads to tempering of the material and softening of the surface layer. Possibly, the formation of microscopic points where the metal is molten. From these zones of molten metal, spraying into the interaction chamber occurs. All of it results in destruction of surface of the first wall and contamination of plasma [4].

Also, in the process of work a thermonuclear reactor, the surface of the first wall is irradiated with fast neutrons (14.2 MeV, ~2 dpa) and nuclear fusion products. In addition, in the process of work of the reactor, helium flows of various intensity appear, which also change the structure of the crystal lattice of the material of the first wall. Therefore, when choosing the material of the first wall, they are guided by the melting temperature of the material. The second parameter for determining the material of the first wall is the change in the material as a result of exposure to nuclear fusion products. That is, it is necessary to know how the lattice structure of the material changes due to the appearance, accumulation and migration of lattice defects. It is also necessary to know how the orientation of the material structure changes as a result of the action of thermonuclear fusion products.

Violation of the thermonuclear reactor first wall material structure changes both the thermal characteristics of the material and the mechanical properties (hardness, plasticity, etc.). In addition, the characteristics of flecking and blistering on the surface of the material change. There is a change in the characteristics of spraying material from the surface.

As perspective materials, for creation of the first wall of thermonuclear reactor, a few types of materials were examined. Among them: ceramics which was covered by a refractory metal; composite metals; tungsten. Our choice was stopped for a tungsten, as on material which possesses the row of specific properties. Tungsten has a high temperature of melting. It is durable at high temperatures. Tungsten has significant residual strength after cooling. Also, tungsten has a high thermal conductivity and a low coefficient of erosive sputtering. It weakly retains tritium. That is, tungsten has a number of specific properties that make it possible to use tungsten as a material for the first wall of a thermonuclear reactor [3–6]. These properties of tungsten are also necessary when it is used in the construction of storage RAW [7], the creation of radiation-protective materials [8–10].

PURPOSE OF WORK

The task of the work is: a) study of effects which arise as a result of affecting of helium ion beams on the surface of tungsten; b) comparison of the macroscopic characteristics of surface of tungsten before irradiation and after irradiation.

THE MAIN PART

One of the technological and effective methods of analysis is the simulation method. For our case, helium ion beams with different energies were used. Helium is slightly soluble in tungsten. When it acts on the surface of tungsten, significant changes in the structure of the tungsten lattice occur. Grates defects appear, which change various characteristics of tungsten (hardness, strength, thermal conductivity). It should be noted that in the case of studying samples from real reactors, questions of residual radioactivity arise.

Simulation allows you to avoid working with radioactive substances. Helium has low solubility in tungsten. Helium exposure leads to strong grate defects.

It becomes possible to obtain the results of changing the grate in a short time. These changes in the grate of tungsten under real conditions must be expected for several years. Therefore, simulation modeling by ion beams makes it possible to study the development and change of defects of grate of surface of tungsten.

To irradiate tungsten with beams of charged ions, a helium ion accelerator was used [11–15]. The accelerator had the following operating characteristics (4 MeV): pulse current up to 1 mA, pulse length 500 μs, repetition frequency 2…5 imp./s, beam diameter on the target 1 cm. Samples are irradiated in the mode when the temperature does not exceed 380 K. That is, experimental studies were carried out in cold conditions. This makes it possible to understand the mechanisms of radiation damage. The contributions of radiation and thermal factors to these damages were separated. When determining the thermal effect of the beam, an IR radiometric method was used to control the beam parameters [16]. This accelerator allows you to perform research with low and high energy helium ions. Beam energy: 0.12 MeV (in injection mode), 4 MeV (in acceleration mode). This allows you to significantly expand the range of research. To diagnose a helium ion beam, it is possible to use gamma-radiation detectors based on mercury compounds [17].

When exposed to helium ions on the surface of a tungsten target, lattice defects appear. These defects have the form of pores [18–21]. The appearance of these defects leads to a change in the characteristics to the surface of tungsten. It is necessary to determine the dynamics of the development of these defects, to find how these defects interact with the surface structure. The study of changes in the structure makes it possible to determine the dynamics of the development of defects. When irradiating the surface of tungsten with a beam of helium ions, an increase in wear resistance, strength, and hardness is possible. The performance characteristics of the material of the first wall are changed. During an irradiation the stream of ions there is their penetration deep into of superficial layer of tungsten target on the depth of ten and hundreds of nanometers [18–21]. As a result of irradiation, defects are formed, and their diffusion occurs. In this case, certain processes occur, which are caused by ion-atomic and ion-electron interactions [21]. In this case, it is possible to predict the resistance of tungsten as the material of the first wall of a thermonuclear reactor.

Two types of tungsten samples were used as a target. The tungsten was of high purity. We designated them W-1 and W-n. The concentration of impurities in tungsten was determined using X-ray fluorescence analysis. Tungsten W-1 contained 99.5% tungsten. Its composition is given in Table 1 a [19]. Tungsten W-n contained 99.7% tungsten and had the following composition (Table 1 b) [19].

All experiments and calculations were performed for the tungsten of type of W-1 and for the tungsten of type of W-n. The results differ slightly. Therefore, the results are given only for the tungsten of type of W-1.

Pucks 2 mm thick and 10 mm in diameter were used as targets. The use of samples of this form makes it possible to obtain the manifestation of all the effects of irradiation on the surface of the sample, from the irradiation side.

Irradiation of samples at a helium ion accelerator is a laborious and time-consuming task. Therefore, we use mathematical modeling. The main calculations were performed using the SRIM code [22]. The calculations of weakening of ionizing radiation were also executed by the code of Geant4 v 4.9.6p02 [23].

The SRIM software package allows, by numerical methods, to obtain the path lengths of various ions in materials. Also, the SRIM software package makes it possible to determine the following characteristics: the distribution of vacancies at the target, the distribution of recoil atoms, etc. It can be used to calculate the characteristics of the movement of ions and their stopping in a wide energy spectrum (up to 2 GeV). The SRIM package is based on the use of the Monte Carlo method. The SRIM package considers quantum-mechanical approximations of ion-atom collisions.

Also, using the SRIM software package, you can calculate the final 3D distribution of ions over the target volume. It is possible to determine the characteristics that depend on the energy losses of the ions. These characteristics are: a) target damage, b) sputtering of target atoms, c) ionization of the target volume, d) phonon production. All these quantities make it possible to determine how the characteristics of the surface of tungsten change.

All studies were carried out in the temperature range of 330…340 K. For helium ions with an energy of 0.12 MeV, the irradiation dose was $1.7 \cdot 10^{18}$ ioн/cm^2. The radiation damage dose was 93.78 dpa.

One of the important parameters is the spray coefficient. On its basis, it is possible to determine how the characteristics of the surface of the material of the first wall and diverter of a thermonuclear reactor change. The sputtering factor is calculated on the basis of cascades of scattering and reflection, which return on a surface.

Therefore, for calculations, we consider a thin surface layer. For cascades, we consider the approximation of scattering on hard spheres. The values of connection energy and displacement energy were used in the calculations. The values of the surface binding energy were also used. These values were considered for each element that is part of tungsten.

The parameter – “sputter yield” is used in determining the spray coefficient. The “sputter yield” parameter is defined as the average number of target atoms per one incident ion. A dose of $5 \cdot 10^6$ helium ions was used in calculations. Atomic sputtering coefficients were obtained for sample W-1 (Table 1). The sputtering coefficients of atoms are given depending on the thickness of the samples. The energy of helium ions is 0.12 MeV.

The total sputtering coefficient was SK $\approx 2 \cdot 10^{-2}$ atom/ion. Sputtering coefficient in the table are given taking into account the accumulation over depth. Distributing of the sputtering coefficient (SK) on spatial intervals was got. This information is resulted.

The first column is the thickness of the layer and the depth of its location.

Tables 1, 2 refer to W-1 tungsten. Component of tungsten makes the main contribution to the sputtering efficiency. The total sputtering coefficients (∑) were obtained after processing Tables 1, 2.

Table 1

Sputter coefficients (sk). Sample W-1
($k \cdot 10^{-5}$ atom/ion, E_{He^+} = 0.12 MeV, density =19.275)

Additives	Thickness	targets	Å	Å
	5	20	40	60
(W-1)	327.7	1480	1790	1940
(Al)	0.1	0.7	0.8	0.9
(Cr)	0.5	1.3	2.3	2.3
(Ni)	0	0.9	0.3	0.9
(Co)	0.1	0.6	0.7	1.0
(Mo)	0.1	1.0	1.4	1.9
(Mn)	0	0.4	0.5	0.6
(Ca)	0.2	1.0	0.8	0.6
(Si)	0	0.4	0.5	0.4
(Pb)	0	1.1	1.1	0.9
(O)	1.3	7.1	6.5	8.4
(Mg)	0	0	0	0
(S)	0.2	0	0.1	0.1
(P)	0.1	0.1	0.2	0.4
(∑)	**330.3**	**1494.6**	**1805.2**	**1958.4**

Table 2

Sputter coefficients depending on the thickness of the layer and the depth of its location. Sample W-1

1(Å)	(W-1)	(∑)
0…2.5	327.7	**330.3**
2.5…7.5	583.9	**589.1**
7.5…12.5	358.4	**362.3**
12.5…17.5	210.0	**212.3**
17.5…22.5	220.0	**219.4**
22.5…27.5	10	**9.5**
27.5…32.5	40.0	**41.8**
32.5…37.5	40.0	**39.9**
37.5…42.5	40.0	**42.2**
42.5…47.5	40.0	**47.8**
47.5…52.5	40.0	**41.5**
52.5…57.5	30.0	**31.7**

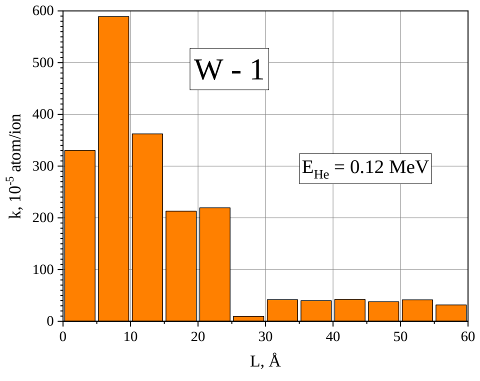

Fig. 1. Change in the total sputtering coefficient (∑) with respect to the depth of the samples: (tungsten type W-1). Irradiation with helium ions with an energy of 0.12 MeV

The total sputtering coefficients (∑) depend on the layer depth. The energy of helium ions was 0.12 MeV. Sputtering coefficients (∑) are shown in Fig. 1.

Helium ions make the main contribution to the sputtering efficiency. Helium ions interact with tungsten in thicknesses up to 25 µm. Integral sputtering characteristics were obtained to study the sputtering coefficient (Fig. 2).

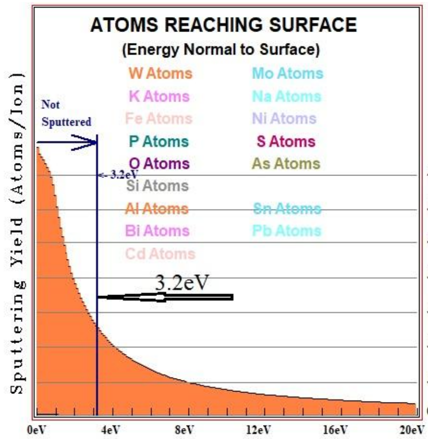

Fig. 2. Integral sputtering characteristics: (tungsten type W-1). Irradiation with helium ions with an energy of 0.12 MeV

The graphs represent the energy of each recoil atom that reaches the surface of the sample. The number of these atoms, in terms of a helium ion, is given along the vertical axis. That is, on the vertical axis, we have a sputtering coefficient. The straight lines 3.2 eV (W-1) and 3.8 eV (W-n) represent the average surface binding energies for these samples. To the left of these straight lines (the Not Sputtered region) are atoms that have an energy below the surface binding energy. Accordingly, these atoms are not sputtered from the surface. To the right of these straight lines are atoms that have reached the surface with energies higher than the surface binding energy. That is, these are the atoms that contribute to the sputtering coefficient.

The integral curves (see Fig. 2) are given for the ideal case. The surface of tungsten has changed after irradiation. The type of surface of tungsten after irradiation is shown in Fig. 3.

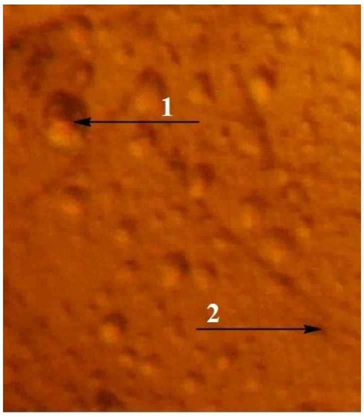

Fig. 3. The surface of tungsten that was irradiated with helium ions with an energy of 0.12 MeV (flux density $1.1 \cdot 10^{18}$ ion/cm^2, 50 dpa)

Fossulas are visible on the surface (flaking phenomenon). Bubbles are visible on the surface (blistering phenomenon). The bubbles didn't burst. There are 20 times fewer bubbles than pits. Elongated filaments of tungsten (tungsten “moss”) form at the edges of the bubbles. These inhomogeneities increase during irradiation. It is quite likely that simultaneously with the irradiation, the process of oxidation of the surface material [24] with the formation of new compounds occurs, which causes differences with the process in the depth of the target. Detachment of the material from the target surface can occur as a result of the occurrence of peak temperatures in the vicinity of zones with accumulated defects [25, 26]. Therefore, the sputtering efficiency increases due to the change in the surface binding energy. The surface binding energy decreases with exposure time. The graphs shown in Fig. 2 allow one to estimate how the sputtering coefficients change when tungsten is irradiated with helium ions. Differential characteristics of the sputtering of atoms on the surface of tungsten were obtained. They are shown in Fig. 4.

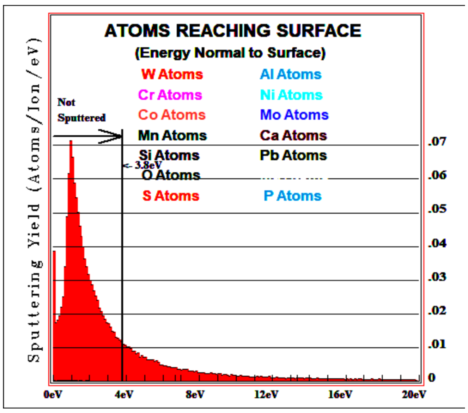

Fig. 4. Differential characteristics of sputtering (tungsten of type of W-1). Irradiation with helium ions with energy 0.12 MeV

They were found for samples of tungsten with different purity. Based on these differential characteristics (see Fig. 4), we can determine with what energy the atoms reach the tungsten surface. Atoms whose energy is less than 3.8 MeV (tungsten of W-1), or less than 3.2 MeV (tungsten of W-n), are not sputtered from the tungsten surface. The sputtering coefficient depends on the helium ion path length (the graph is shown in Fig. 5).

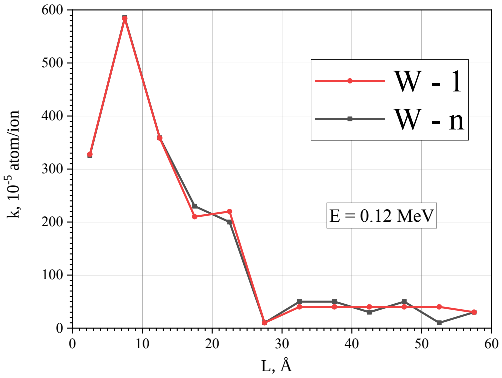

Fig. 5. Change of the sputtering coefficient depending on the length of the helium ion range

The count of atoms is given in the amount per helium ion. The maximum number of atoms is sputtered in the range of mean free paths from 0.03 to 0.13 µm. The sputtering peak ($590\cdot10^5$ atom/ion) is at a depth of 0.07…0.08 µm. At depths of 0.27…0.57 µm, no more than $(40…50)\cdot10^5$ atom/ion is sprayed. This is no more than 10% of the maximum value of atoms. The structure of the target material changes along the path of the helium ions. In this case, tungsten is ionized, phonons are formed, vacancies appear, and segregation (redistribution) of atoms occurs. Graphs of changes in these characteristics are presented on Fig. 6.

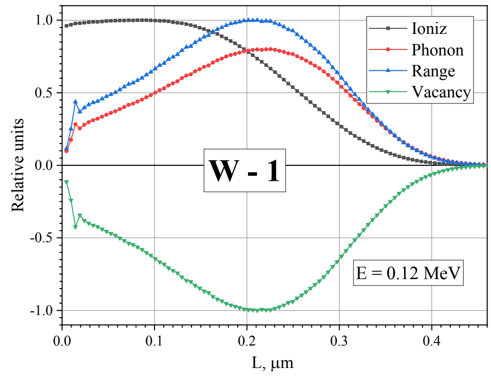

Fig. 6. Graphs of changes in characteristics. Irradiation with helium ions with energy 0.12 MeV (tungsten of type of W-1)

The graphs show that the maximum photon yield (red line) was found in the 0.2 µm region. There is maximal appearance of vacancies at these lengths of free run (green line). Also, in this area, there is a redistribution (segregation) of atoms (dark blue line). The results are almost the same for both tungsten of type of W-1 and tungsten of type of W-n. The results obtained are consistent with the results presented in Fig. 5. In the region of 0.2 µm, we observe a plateau.

Damage coefficients were obtained for the tungsten of type of W-1 and the tungsten of type of W-n. Irradiation with helium ions with energies of 0.12 MeV. Graphs Fig. 6 was used to calculate the damage factor dpa (dpa is the number of displacements per atom) and the profiles over which the damage factor is distributed.

The final expression for calculating displacements per atom (dpa) looks like:

$$dpa = \frac{D_{ion}\cdot dpi}{N_A\cdot\rho_0\cdot SL}\cdot\frac{1}{100}\sum_i \mu_i n_i\,, \qquad (1)$$

D_{ion} – is the radiation dose [ion/cm^2]. The D_{ion} parameter is found from the experimental conditions. The *dpi* parameter – is the number of displacements per ion. It is found from the total number of displacements per ion (from SRIM calculations, see Tables 1, 2). Also, N_A – is the Avogadro number, $m_{mole} = m/M$, $m = \rho_0 \times SL$. In this equation, ρ_0 – is the density of the sample, which was measured experimentally. S =1 cm^2 – is the unit area of the sample, L – is the maximum range of ions in the sample. The value $M = 1/100\times\sum\mu_i n_i$ – is the molar mass of the sample. The value of μ_i – is the molecular weight of the *i*-th element of the sample, n_i – is the percentage of the *i*-th element of the sample.

Using expression (1), the damage profiles of samples of tungsten were obtained (Fig. 7).

The radiation dose was $1 \cdot 10^{18}$ ion/cm^2. The energy of helium ions was 0.12 MeV. The damage rate was dpa ≈ 60. The half-width of the displacement peak is in the range from 0.1 to 0.3 μm. The displacement peak is located at the point, where length of free run is equal 0.2 μm. This point coincides with the location of peaks, phonon profiles, and vacancies.

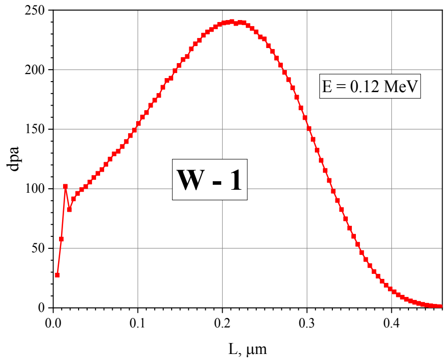

Fig. 7. Displacement formation profiles in samples of tungsten (tungsten of type of W-1). Irradiation with helium ions with energy 0.12 MeV

CONCLUSIONS

1. The samples of tungsten were irradiated with helium ions with energies of 0.12 MeV. Samples of different percentages were irradiated.

2. Total sputtering ratios calculated for W-1 and W-n samples of tungsten. The total sputtering coefficients are determined by the amount of tungsten and weakly depend on other elements.

3. The calculation of the total coefficients must be carried out to depths of 60 Å.

4. Damage profiles and damage coefficients have been obtained, which makes it possible to predict the wear of tungsten in the process of exploitation.

5. It was found that there are 20 times more pits on the surface of sample than bubbles.

6. It was found that 95% of the energy of helium ions is spent on tungsten ionization ($E_{He}{}^{+}$ = 0.12 MeV). Vacancies and phonons are formed due to displacement cascades.

REFERENCES

1. C.H. Wu, C. Alessandrini, et al. Progress of the European R&D on plasma-wall interactions, neutron effects and tritium removal in ITER plasma facing materials // *Fusion Engineering and Design*. 2001, v. 56-57, p. 179-187.
2. H Yu et al. Hardening and Strain Localisation in Helium-Ion-Implanted Tungsten // *Scientific Reports*. 2019. 9:18354, https://doi.org/10.1038/s41598 019-54753-3
3. I.E. Garkusha et al. // *Fusion Sci. Technol.* 2014, v. 65(2), p. 186.
4. T. Hirai et al. Use of tungsten material for the ITER divertor // *Nuclear Materials and Energy*. 2016, https://dx.org/10.1016/j.nme.2016.07.003.
5. M. Rieth et al. Recent progress in research on tungsten materials for nuclear fusion applications in Europe // *J. Nucl. Mater*. 2013, v. 432, p. 482-500.
6. S.Pestchaniy et al. Estimation of the dust production rate from the tungsten armour after repetitive ELM-like heat loads// *Physica Scripta*. 2011, v. 145, p. 014062.
7. V.F. Klepikov, E.M. Prokhorenko, V.V. Lytvynenko, S.E. Donets, V.N. Robuk, T.G. Prokhorenko, V.T. Uvarov, A.G. Ponomarev, Yu.F. Lonin. The use of high-current relativistic electron beams for the study of the effects of ionizing radiation on materials storage RAW // *Problems of Atomic Science and Technology*. 2016, № 2(102), p. 72-77.
8. E.M. Prokhorenko et al. Improving of characteristics of composite materials for radiation biological protection *// Problems of Atomic Science and Technology. Series "Nucl. Phys. Inv. (61)".* 2013, №6(88), p. 240-243
9. V.F. Klepikov, E.M. Prokhorenko, V.V. Lytvynenko, A.A. Zaharchenko, M.A. Hazhmuradov. Performance Ratio Hardness Characteristics Polystyrene-Metal Composite Materials // *Problems of Atomic Science and Technology*. 2015, № 5(99), p. 36-42.
10. E.M. Prohorenko et al. Metal containing composition materials for radiation protection. // *Problems of Atomic Science and Technology.* 2014, № 4(92), p. 125-129.
11. S.N. Dubniuk, B.V. Zajtsev. The linear ace- lerator for radiation structural materials // *Problems of Atomic Science and Technology*. 2014, № 3, p. 172-176.
12. R.A. Anokhin, B.V. Zaitsev, K.V. Pavlii, V.G. Zhuravlev, V.A. Soshenko. Experimental complex for investigation of construction materials on the helium ions linear accelerator // *Problems of Atomic Science and Technology*. 2017, № 6(112), p. 167-171.
13. S.N. Dubniuk, R.A. Anokhin, A.F. Dyachenko, A.P. Kobets, A.I. Kravchenko, O.V. Manuilenko, K.V. Pavlii, V.N. Reshetnikov, A.S. Shevchenko, V.A. Soshenko, S.S. Tishkin, B.V. Zajtsev, A.V. Zhuravlyov, V.G. Zhuravlyov. Radiation complex on the basis of helium ions linac // *Problems of Atomic Science and Technology.* 2018, № 4(116), p. 46-51.
14. V.I. Butenko, S.N. Dubniuk, A.F. Dyachenko, A.P. Kobets, O.V. Manuilenko, K.V. Pavlii, V.A. Soshenko, S.S. Tishkin, B.V. Zajtsev. Constructional materials experimental researches on the helium ions linear accelerator // *Problems of Atomic Science and Technology*. 2021, № 4(134), p. 85-89, https://doi.org/10.46813/2021-134-085
15. I.M. Onishchenko, O.V. Manuilenko, B.V. Zajtsev, S.M. Dubniuk, A.P. Kobets, A.I. Kravchenko, K.V. Pavlii, V.M. Reshetnikov, V.A. Soshenko, S.S. Tishkin, O.V. Zhuravlyov, V.G. Zhuravlyov. Experimental research and work development on the helium ions linac // *Problems of Atomic Science and Technology*. 2021, № 6(136), p. 197-200, https://doi.org/10.46813/2021-136-197
16. E.M. Prohorenko, V.F. Klepikov, V.V. Lytvynenko, N.I. Bazaleyev, I.I. Magda, T.G. Prohorenko, A.I. Morozov. Application of ir-radiometric diagnostics for control of vacuum connections of electrophysical installations // *Problems of Atomic*

Science and Technology. 2018, № 1(113), p. 212-217.

17. A.A. Zakharchenko et al. Simulation of characteristics of gamma-radiation detectors based on mercury compounds // *Problems of atomic Science and Technology. Series "Nucl. Phys. Inv. (60)"*. 2013, № 3(85), p. 231-235.
18. D. Nishijima, M.Y. Ye, N. Ohno, and S. Takamura. Formation mechanism of bubbles and holes on tungsten surface with low-energy and high-flux helium plasma irradiation in NAGDIS-II // *J. Nucl. Mat*. 2004, v. 329-333, p. 1029-1033.
19. O.V. Manuilenko, E.M. Prokhorenko, K.V. Pavlii, B.V. Zajtsev, S.N. Dubniuk, V.V. Lytvynenko, T.G. Prokhorenko. Changes of the radiation characteristics of surface of tungsten as a result of influence of helium ion beams // *Problems of Atomic Science and Technology*. 2022, № 3(139), p. 36-41, https://doi.org/10.46813/2022-137-122.
20. M. Baldwin, R. Doerner. Helium induced nanoscopic morphologhy on tungsten under fusion relevant plasma conditions // *Nucl. Fusion*. 2008, v. 48, p. 035001–5.
21. S Sharafat et al. A description of stress driven bubble growth of helium implanted tungsten // *Journal of Nuclear Materials*. 2009, v. 389, p. 203-212, https://doi.org/10.1016/j.jnucmat.2009.02.027
22. http://www.srim.org.
23. V.F. Klepikov, E.M. Prokhorenko, V.V. Lytvynenko, A.A. Zaharchenko, M.A. Hazhmuradov. Application of methods of modeling of radiation-protective characteristics of polystyrene-metal composite materials // *Problems of Atomic Science and Technology*. 2016, № 3(103), p. 123-127.
24. V.V.Bryukhovetsky et al. The features of the structural state and phase composition of the surface layer of aluminum alloy Al-Mg-Cu-Zn-Zr irradiated by the high current electron beam // *Nuclear Inst. and Methods in Physics Research, B*. 2021, v. 499, p. 25-31.
25. V.V.Bryukhovetskij et.a. / Effect of the pulsed electron irradiation on superplasticity properties of duraluminum // *Fizika i Khimiya Obrabotki Materialov*. 2002, v. 4, p. 33-38.
26. A.Yu. Didyk et al. Change in sample surface area during formation of cylindrical tracks as a result of high-energy heavy-ion irradiation // *Metallofizika i Noveishie Tekhnologii*. 2010, v. 32(3), p. 357-363 (in Russian).

Article received 11.02.23

ВПЛИВ ПУЧКІВ ІОНІВ ГЕЛІЮ З ЕНЕРГІЯМИ 0,12 МеВ НА ПРОЦЕС РОЗПИЛЕННЯ НА ПОВЕРХНІ ВОЛЬФРАМУ

О.В. Мануйленко, Є.М. Прохоренко, К.В. Павлій, Б.В. Зайцев, С.М. Дубнюк, В.В. Литвиненко, Ю.О. Касаткін, Т.Г. Прохоренко

Проведено опромінення зразків вольфраму з чистотою 99,5 і 99,7% пучками іонів гелію (E_{He}^{+} = 0,12 МеВ). Отримано сумарні коефіцієнти розпилення за глибиною зразка до 60 Å від поверхні зразка. Знайдено, що на поверхні зразків вольфраму кількість ямок (ефект флекінгу) істотно перевищує кількість бульбашок (ефект блістерингу). Пораховані профілі пошкодження поверхні вольфраму в результаті опромінення іонами гелію. Визначено зони максимального прояву руйнівних ефектів.